Korean J. Chem. Eng., 32(8), 1477-1485 (2015)
DOI: 10.1007/s11814-014-0369-8

pISSN: 0256-1115
eISSN: 1975-7220

Performance simulations of MEA/NH_3 based large-scale CO_2 capture in packed columns under different flue gas parameters

Minkai Zhang and Yincheng Guo†

Department of Engineering Mechanics, Tsinghua University, Beijing 100084, China
(*Received 9 July 2014 • accepted 8 December 2014*)

Abstract−Based on the rate-based process simulation, performances of MEA and NH_3 based large-scale CO_2 capture in packed columns under different flue gas parameters were investigated. Simulation results show that the CO_2 regeneration energy for the MEA based process is lower than that for the NH_3 based process, which is mainly because the flow rate of the MEA solution is significantly lower than that of the aqueous ammonia. The MEA leakage concentration is far lower than the NH_3 leakage concentration, and this indicates that the NH_3 abatement system should be added for dealing with the NH_3 slip in the NH_3 based CO_2 capture process. With the flow rate of the flue gas increasing, the liquid gas ratios for both processes decrease, which gives rise to the decrease of the CO_2 removal efficiencies for the two processes. Since the liquid gas ratios are very high, the temperature of the flue gas has little effects on the MEA and NH_3 based CO_2 capture processes. The comparative studies on the effects of the flue gas parameters can provide technical guidance for the pretreatment of the flue gas before CO_2 capture.

Keywords: CO_2 Capture, MEA, Aqueous Ammonia, Flue Gas, Packed Column, Rate-based Simulation

INTRODUCTION

Post-combustion CO_2 capture with the chemical absorption method is considered as a feasible way for mitigating the huge CO_2 emissions from coal-fired power plants [1]. Categorized by the absorbent, the chemical absorption methods for CO_2 capture from the flue gas of coal-fired power plant mainly include the MEA [2] and NH_3 [3] based processes. The MEA based CO_2 capture process has been applied to capture CO_2 from the flue gas in pilot-scale power plants due to its high CO_2 reactivity [4,5]. However, it has low CO_2 absorption capacity [6], degradation caused by high temperature, O_2 and acid gases (SO_2, NO_x, and HCl) [7], corrosive problems [8], and high energy requirement for regeneration [9]. Accordingly, the NH_3 based process is considered as a promising alternative due to its high CO_2 absorption capacity, no degradation and corrosion, and simultaneous capture of CO_2, SO_2, and NO_x [1,10].

Currently, most studies on the MEA and NH_3 based CO_2 capture processes focus on small-scale applications, while those at a scale of 1 million tons CO_2 captured annually at a capture efficiency of 90% are less investigated [11]. From the long run, only the large-scale CO_2 capture can actually mitigate the CO_2 emissions from the power plants significantly. For the large-scale CO_2 capture, experimental studies need large capital costs and are not suitable for the initial technology development, while process simulations provide an economical and convenient method. Categorized by the description of heat/mass transfer, there are two models for simulating the MEA and NH_3 based processes, namely the equilibrium- and rate-based models. The equilibrium-based model assumes that the vapor and liquid phases leaving every stage reach equilibrium, while the rate-based model considers the actual heat/mass transfer rates and assumes the equilibrium of the vapor and liquid phases only exists at their interface [12]. If using the equilibrium-based model, the overestimated heat/mass transfer rates can lead to overestimated CO_2 absorption rate and correspondingly higher CO_2 loading of the rich solvent flowing out of the absorber. This can further result in lower regeneration energy due to that the rich solvent directly flows into the stripper after the heat-exchanger and heater, and it needs less energy for regenerating the same amount of CO_2 if its CO_2 loading is higher. The regeneration energy predicted by Duan et al. [13] with the equilibrium-based model is significantly lower than that predicted by Zhang and Guo [14] with the rate-based model and the experimental results from the Munmorah pilot plant [15]. The rate-based model is more appropriate for simulating the MEA and NH_3 based CO_2 capture processes, which has been confirmed by Zhang et al. [16] for the MEA based process, and Ghaemi et al. [17] for the NH_3 based process.

The MEA solution and aqueous ammonia represent two typical absorbents for the chemical absorption method, and therefore their comparative studies can give technical guidance for selecting which one for the large-scale CO_2 capture. However, previous comparative studies on the two processes mainly focus on the mass transfer ability [18,19], absorption rate [20], CO_2 removal ability [21-23], absorption capacity [21,24,25], and regeneration energy [15, 26]. Puxty et al. [18] reported that the overall mass transfer coefficients for the 5 mol/L MEA solution at 40 °C and 60 °C were 1.5-2 times larger than those for the 6 mol/L aqueous ammonia at 20 °C. Dave et al. [19] reported that at the same CO_2 loading, the overall mass transfer coefficients for the 30 wt% MEA solution at 40 °C were approximate to those for the 10 wt% aqueous ammonia at

†To whom correspondence should be addressed.
E-mail: guoyc@tsinghua.edu.cn

20 °C. Hsu et al. [20] compared the absorption rates of CO_2 into the MEA solution and aqueous ammonia and found that, in general, the absorption rate of CO_2 into the MEA is higher than that of CO_2 into aqueous ammonia. Yeh and Bai [21] reported that the maximum CO_2 removal efficiency by aqueous ammonia can achieve 99%, while under the same operating conditions, the maximum CO_2 removal efficiency is 94% by MEA. Niu et al. [22] compared the capture efficiencies of CO_2 by fine spray of MEA solution and aqueous ammonia and found that under comparable conditions and with the same absorbent concentrations, the CO_2 removal efficiency of using MEA solution is lower than that of using aqueous ammonia due to the larger stoichiometric ratio of MEA to CO_2. Pellegrini et al. [23] also confirmed the superiority of aqueous ammonia on CO_2 removal ability. Yeh and Bai [21], Ma et al. [24], and Rivera-Tinoco and Bouallou [25] all reported that comparing to the MEA solution, aqueous ammonia has a higher CO_2 absorption capacity, and the maximum CO_2 absorption capacity of aqueous ammonia is three times of that of MEA solution [21]. The lowest regeneration energy reported from the Munmorah pilot plant (4.0-4.2 MJ/kg CO_2) for the NH_3 based process is higher than the typical regeneration energy (3.7 MJ/kg CO_2) for the MEA based process [15], but after the optimization by Zhang and Guo [26] using the rate-based process simulations, the regeneration energy can be lower than that for the MEA based process.

Although there are many papers discussing the comparisons of the two processes, effects of the flue gas parameters such as the flow rate, temperature and CO_2 concentration on the two processes in packed columns are less focused. The difference of the coal combustion due to the different qualities of coal and its combustion process and following desulfurization, denitration and cooling operations can all lead to the change of the flow rate, temperature, and CO_2 concentration of the flue gas, which may further affect the CO_2 capture process. Niu et al. [27] and Ma et al. [28] performed experiments on the laboratory-scale MEA and NH_3 based processes, respectively, and found that the increase of flow rate of the flue gas or its CO_2 concentration will both lead to the decrease of the CO_2 removal efficiency when keeping the concentration of absorbent constant. But, these experiments only focused on the small-scale MEA and NH_3 based CO_2 capture processes. Meanwhile, effects of flue gas parameters on the solvent leakage, CO_2 output and regeneration energy were not included in these comparisons [18-26]. Here, the CO_2 output is the flow rate of CO_2 in the gas product flowing out of the stripper. Besides, the reaction column is also a critical consideration for the MEA and NH_3 based process. Puxty et al. [18] and Dave et al. [19] measured the overall mass transfer coefficient using a wet-wall column. Hsu et al. [20] measured the absorption rate with a stirred vessel. Yeh and Bai [21] and Pellegrini et al. [23] measured the CO_2 removal efficiency using a semi-continuous flow reactor. Niu et al. [22] measured the CO_2 removal efficiency with a fine spray column. Ma et al. [24] measured the CO_2 removal efficiency using a bubble reactor. Rivera-Tinoco and Bouallou [25] meansured the CO_2 absorption capacity with a thermostated glass reactor of Lewis-type. However, for actual industrial applications, the packed columns having high separation performance are often adopted. The vapor-liquid mass transfer behavior in packed columns is different from that in wet-wall column, stirred vessel, semi-continuous flow reactor, bubble reactor, and thermostated glass reactor of Lewis-type, and fine spray column. Yu et al. [15] adopted the packed columns but did not consider the effects of flue gas parameters on the two CO_2 capture processes, while the focus is mainly on the NH_3 based CO_2 capture process.

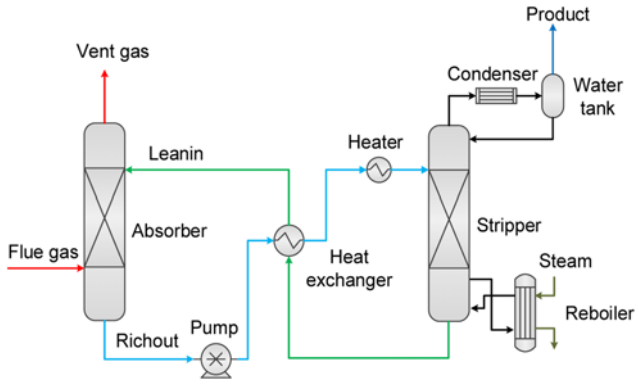

Fig. 1. Simplified flow diagram for the MEA and NH_3 based CO_2 capture processes.

Thus, in this paper, the rate-based process simulations of the large-scale MEA and NH_3 based CO_2 capture processes in packed columns were carried out. Effects of the parameters of the flue gas such as the flow rate, temperature, and CO_2 concentration on the two CO_2 capture processes were investigated and compared. The comparative studies on effects of the flue gas parameters can provide technical guidance for the pretreatment of the flue gas before CO_2 capture.

MEA AND NH_3 BASED CO_2 CAPTURE PROCESSES

Simplified flow diagram for the MEA and NH_3 based large-scale CO_2 capture processes is shown in Fig. 1. For the two processes, the major difference is the absorbent adopted for capturing the CO_2 in the flue gas, in which the MEA based process adopts the MEA solution while the NH_3 based process adopts the aqueous ammonia solution. After the desulfurization, denitration and cooling operations, the flue gas flows into the absorber and contacts countercurrent with the lean absorbent flowing into the absorber from its top. In the absorber, the lean absorbent absorbs the CO_2 in the flue gas and turns into the rich absorbent. Then, the rich solvent directly flows into the stripper after heat-exchanger and heater. Steam is introduced for regenerating the rich solvent and the regenerated CO_2 is used for the following storage or utilization. The absorbers in the MEA and NH_3 based CO_2 capture processes are often operated at the normal pressure. This is particularly appropriate for large-scale CO_2 capture process because the flow rate of the flue gas is very high and it will cost too much energy for compressing the flue gas. The stripper in the MEA based CO_2 capture process can be operated at significantly or slightly evaluated pressures [13,29]. This stripper in the NH_3 based process can also be operated at the normal pressure or significantly evaluated pressures [14,15]. Compared with the evaluated pressures, regeneration at normal pressure can reduce the regeneration temperature and further reduce the requirement for the steam from the power plant. In this paper, the absorber

Table 1. Parameters of part of the full flue gas from a typical 500 MW coal-fired power plant

Flow rate, kg/s	Pressure, kPa	Temperature, °C	Volume concentration, vol%			
			N_2	CO_2	H_2O	O_2
185.7	101.3	50.0	71.29	12.43	11.84	4.44

Table 2. Properties of the absorbents for the MEA and NH_3 based large-scale CO_2 capture processes

Absorbent	Flow rate, m^3/s	Concentration, $mol \cdot L^{-1}$	CO_2 loading, $[C]_{mol}/[N]_{mol}$	Pressure, kPa	Temperature, °C
MEA solution	0.495	MEA: 5.0	0.23	101.3	38
Aqueous NH_3	2.050	NH_3: 3.0	0.23	101.3	38

and stripper are both operated at the normal pressure.

In addition, according to the rate-base process simulations of the NH_3 based large-scale CO_2 capture process reported by Zhang and Guo [14], both the absorber and stripper adopt packed columns, and the packing material is DZ-II-750Y packing. The inner diameter and packed height of the absorber are 12.0 m and 20.0 m, respectively. The inner diameter and packed height of the stripper are 10.0 m and 12.0 m, respectively. In the MEA and NH_3 based processes, the condenser temperatures are both set as 30 °C while the boilup ratios are set as 0.17 and 0.35, respectively. Here, the boilup ratio is the vapor flow rate at the last stage to the bottom liquid product [12]. For the two processes, the temperatures of the rich solvents flowing into the stripper are both set as 90 °C.

For the full flue gas from a typical 500 MW coal-fired power plant, the absorber will be too huge if keeping the CO_2 removal efficiency above 90% [14], and therefore Zhang and Guo [14] suggested capturing part of the full flue gas. Since there is no fully verified or commercialized CO_2 capture process at the scale of 1 million tons CO_2 captured annually at a capture efficiency of 90% at present [11], we considered part of the full flue gas after the desulfurization, denitration and cooling operations from a typical 500 MW coal-fired power plant. According to Ref. [30], the parameters of part of the full flue gas are shown in Table 1, if keeping the CO_2 removal efficiency as 90%, the CO_2 captured annually can reach 1 million tons. When studying the effects of the parameters of the flue gas, if one of the flow rate, temperature, and CO_2 concentration changes, the other two are assumed unchanged. When changing the CO_2 concentration in the flue gas, we keep the sum of the volume concentrations of N_2, CO_2, H_2O and O_2 as 1.0 by adjusting the N_2 concentration.

The properties of the absorbents for the MEA and NH_3 based large-scale CO_2 capture processes are shown in Table 2. The MEA solution adopted the typical 30 wt% MEA solution, while the aqueous ammonia adopted the optimized concentration 3.0 $mol \cdot L^{-1}$ [14]. Their CO_2 loading and temperature of the two absorbents also referred to Ref. [14]. Their flow rates are determined by using the rate-based model built in the next section. Under these flow rates, the CO_2 removal efficiencies of the two CO_2 capture processes can both reach 90%. Besides, although the chilled ammonia process was developed by Alstom for dealing with the NH_3 slip problem, it still suffers precipitation problem and high energy requirement for chilling the flue gas and absorbent [31]. Also, if adopting the chilled ammonia process, it still needs the NH_3 abatement system for reducing the NH_3 leakage concentration to the environmental requirement [31]. Thus, in this paper, the aqueous ammonia adopted the optimized absorbent temperature 38 °C in Ref. [14].

RATE-BASED MODEL

1. Model Specification

The rate-based model was built for simulating the MEA and NH_3 based CO_2 capture processes. The core of the rate-based model is describing the actual heat/mass transfer and chemical reactions. The Redlich-Kwong equation of state and the Electrolyte-NRTL method are used for computing properties of the vapor and liquid phases, respectively. Detailed descriptions of the Redlich-Kwong equation of state and the Electrolyte-NRTL method can be found in our previous work [32]. In this paper, CO_2, NH_3, and N_2 are seen as the Henry components, and their vapor-liquid equilibriums are described with the Henry's law. Meanwhile, the vapor-liquid equilibrium of the solvent water is described with the Raoult's law. The Henry's constants of CO_2, NH_3, and N_2 are obtained with the following correlation:

$$\ln H_{ij}(T, p) = A_{ij} + \frac{B_{ij}}{T} + C_{ij}\ln T + D_{ij}T + \frac{E_{ij}}{T^2}, \quad (1)$$

in which A_{ij}, B_{ij}, C_{ij}, D_{ij}, E_{ij} are the related parameters, as shown in Table 3. The flow model is set as countercurrent. The liquid holdup is determined by using the method reported by Chen [33], and 4% of the free volume of the column is chosen in this paper. The heat transfer coefficient is estimated with the Chilton-Colburn method

Table 3. Temperature-dependent binary parameters-HENRY

Component i	NH_3	CO_2	N_2
Component j	H_2O	H_2O	H_2O
Temperature units	K	K	K
Property units	Pa	Pa	Pa
A_{ij}	−133.463	170.713	176.507
B_{ij}	−157.552	−8477.71	−8432.77
C_{ij}	28.1001	−21.9574	−21.558
D_{ij}	−0.049227	0.00578075	−0.00843624
E_{ij}	0	0	0
T_{LOWER}	273	273	273
T_{UPPER}	498	500	346

[34]. The mass transfer coefficient and interfacial area are estimated with the empirical correlation formulas developed by Bravo et al. [35]. Other relevant coefficients are obtained from the default correlations in Aspen Plus [12].

There are two models for describing the chemical reactions in the MEA-CO_2-H_2O or NH_3-CO_2-H_2O system: chemistry and kinetic models. For the chemistry model, all chemical reactions are equilibrium reactions. As for the kinetic model, it adds the kinetic reactions of CO_2 with NH_3 and OH^- which describe the chemical reactions more precisely. The absorber and stripper both adopt the kinetic model, except that the condenser and reboiler stages adopt the chemistry model. The settings of the reaction model for the condenser and reboiler are the same with the templates in Aspen Plus [12]. The chemistry and kinetic models for the MEA-CO_2-H_2O and NH_3-CO_2-H_2O systems are shown in Tables 4 and 5, respectively.

Table 4. Chemistry and kinetic models for the MEA-CO_2-H_2O system

Reaction ID	Reaction type	Chemical equation
Chemistry model for the MEA-CO_2-H_2O system		
1	Equilibrium	$2H_2O \leftrightarrow H_3O^+ + OH^-$
2	Equilibrium	$CO_2 + 2H_2O \leftrightarrow HCO_3^- + H_3O^+$
3	Equilibrium	$HCO_3^- + H_2O \leftrightarrow CO_3^{2-} + H_3O^+$
4	Equilibrium	$MEAH^+ + H_2O \leftrightarrow MEA + H_3O^+$
5	Equilibrium	$MEACOO^- + H_2O \leftrightarrow MEA + HCO_3^-$
Kinetic model for the MEA-CO_2-H_2O system		
1	Equilibrium	$MEAH^+ + H_2O \leftrightarrow MEA + H_3O^+$
2	Equilibrium	$2H_2O \leftrightarrow H_3O^+ + OH^-$
3	Equilibrium	$HCO_3^- + H_2O \leftrightarrow CO_3^{2-} + H_3O^+$
4	Kinetic	$CO_2 + OH^- \rightarrow HCO_3^-$
5	Kinetic	$HCO_3^- \rightarrow CO_2 + OH^-$
6	Kinetic	$MEA + CO_2 + H_2O \rightarrow MEACOO^- + H_3O^+$
7	Kinetic	$MEACOO^- + H_3O^+ \rightarrow MEA + CO_2 + H_2O$

Table 5. Chemistry and kinetic models for the NH_3-CO_2-H_2O system

Reaction ID	Reaction type	Chemical equation
Chemistry model for the NH_3-CO_2-H_2O system		
1	Equilibrium	$2H_2O \leftrightarrow H_3O^+ + OH^-$
2	Equilibrium	$CO_2 + 2H_2O \leftrightarrow HCO_3^- + H_3O^+$
3	Equilibrium	$HCO_3^- + H_2O \leftrightarrow CO_3^{2-} + H_3O^+$
4	Equilibrium	$NH_3 + H_2O \leftrightarrow NH_4^+ + OH^-$
5	Equilibrium	$NH_3 + HCO_3^- \leftrightarrow NH_2COO^- + H_2O$
6	Salt	$NH_4HCO_3(S) \leftrightarrow NH_4^+ + HCO_3^-$
Kinetic model for the NH_3-CO_2-H_2O system		
1	Equilibrium	$NH_3 + H_2O \leftrightarrow NH_4^+ + OH^-$
2	Equilibrium	$2H_2O \leftrightarrow H_3O^+ + OH^-$
3	Equilibrium	$HCO_3^- + H_2O \leftrightarrow CO_3^{2-} + H_3O^+$
4	Kinetic	$CO_2 + OH^- \rightarrow HCO_3^-$
5	Kinetic	$HCO_3^- \rightarrow CO_2 + OH^-$
6	Kinetic	$NH_3 + CO_2 + H_2O \rightarrow NH_2COO^- + H_3O^+$
7	Kinetic	$NH_2COO^- + H_3O^+ \rightarrow NH_3 + CO_2 + H_2O$
8	Salt	$NH_4HCO_3(S) \rightarrow NH_4^+ + HCO_3^-$

For the equilibrium reactions, equilibrium constants should be determined. The equilibrium constants for the equilibrium reactions in the MEA-CO_2-H_2O system are calculated by using the standard Gibbs free energy change. The equilibrium constants K_{eq} for the equilibrium reactions in the NH_3-CO_2-H_2O system are calculated using the following correlation [12]:

$$\ln K_{eq} = A + B/T + C\ln(T) + DT, \tag{2}$$

where T is the Kelvin temperature and A, B, C, D are relevant parameters. Here, the relevant parameters are determined according to Ref. [36]. For the kinetic reactions, reaction rates should be determined. The reaction rates of the kinetic reactions in the MEA-CO_2-H_2O and NH_3-CO_2-H_2O systems are determined by the following power law [12]:

$$r = kT^n \exp\left(-\frac{E}{RT}\right)\prod_{i=1}^{N} C_i^{\alpha_i}, \tag{3}$$

where r is the reaction rate, k is the pre-exponential factor, n is the temperature exponent, E is the activation energy, R is the universal gas constant, C_i is the molarity of component i, α_i is the stoichiometric number of component i, and N is the number of components. The parameters of k, n and E in Eq. (3) for the kinetic models of the MEA-CO_2-H_2O and NH_3-CO_2-H_2O systems are shown in Table 6. For the MEA-CO_2-H_2O system, the kinetic parameters for reaction 4 are taken from Pinsent et al. [37], the kinetic parameters for reaction 5 are derived by using the kinetic parameters of reaction 4 and the equilibrium constants of the reversible reactions 4 and 5, and the kinetic parameters for reactions 6-7 are calculated from the work of Hikita et al. [38]. For the NH_3-CO_2-H_2O system, the kinetic parameters for reactions 4-7 are obtained from Pinsent et al. [37].

2. Model Validation

The model validation was carried out for ensuring the effectiveness of the rate-based model. The thermodynamic model was validated using the flash calculations. Since MEA is less volatile, experimental results on vapor partial pressures in the MEA-CO_2-H_2O

Table 6. Parameters of k, n, and E in Eq. (3) for the Kinetic models of the MEA-CO_2-H_2O and NH_3-CO_2-H_2O systems

Reaction ID	k	n	E, KJ·mol^{-1}
Kinetic model for the MEA-CO_2-H_2O system			
4	4.32e+13	0	55.38
5	2.38e+17	0	123.11
6	9.77e+10	0	41.20
7	3.23e+19	0	65.44
Kinetic model for the NH_3-CO_2-H_2O system			
4	4.32e+13	0	55.38
5	2.38e+17	0	123.11
6	1.35e+11	0	48.43
7	4.75e+20	0	69.09

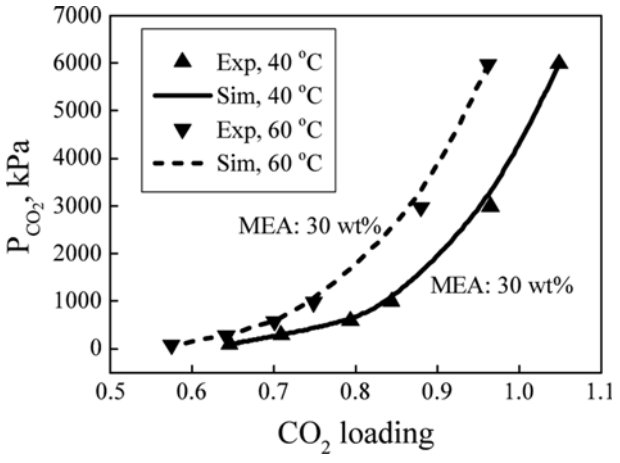

Fig. 2. Comparison of the predicted CO_2 partial pressures at 40 °C and 60 °C in the MEA-CO_2-H_2O system and the experimental results reported by Jou et al. [40].

system usually only focus on the CO_2 partial pressures [39,40]. Fig. 2 shows the comparison of the predicted CO_2 partial pressures at 40 °C and 60 °C in the MEA-CO_2-H_2O system, and the experimental results reported by Jou et al. [40]. But for the NH_3-CO_2-H_2O system, since NH_3 is easy to volatilize, experimental results on vapor partial pressures in this system focus on both the CO_2 and NH_3 partial pressures [41,42]. Fig. 3 shows the comparisons of the predicted CO_2 and NH_3 partial pressures at 60 °C and 80 °C in the NH_3-CO_2-H_2O system, and the experimental results reported by Kurz et al. [41] for 60 °C and Goppert and Maurer [42] for 80 °C. From Figs. 2 and 3, it can be seen that the predicted CO_2 pressures in the MEA-CO_2-H_2O system and CO_2 and NH_3 partial pressures in the NH_3-CO_2-H_2O system all agree well with the experimental results. Thus, the effectiveness of the thermodynamic models used in this paper can be ensured. The effectiveness of the rate-based model established above for the MEA and NH_3 based CO_2 capture processes was also validated, and its details can be found in Refs. [12,14].

Apart from the model validation, the stage number chosen when performing simulations may affect the model outputs after the rate-based model is determined. Fig. 4 shows the predicted CO_2 removal efficiency and CO_2 output in the base scenarios of the large-scale MEA and NH_3 based CO_2 capture processes at different stage numbers. Here, the base scenarios are the same as the operating conditions determined in the previous Section. The larger stage number can give more accurate model outputs, but it is usually more difficult to reach convergence when performing simulations at larger

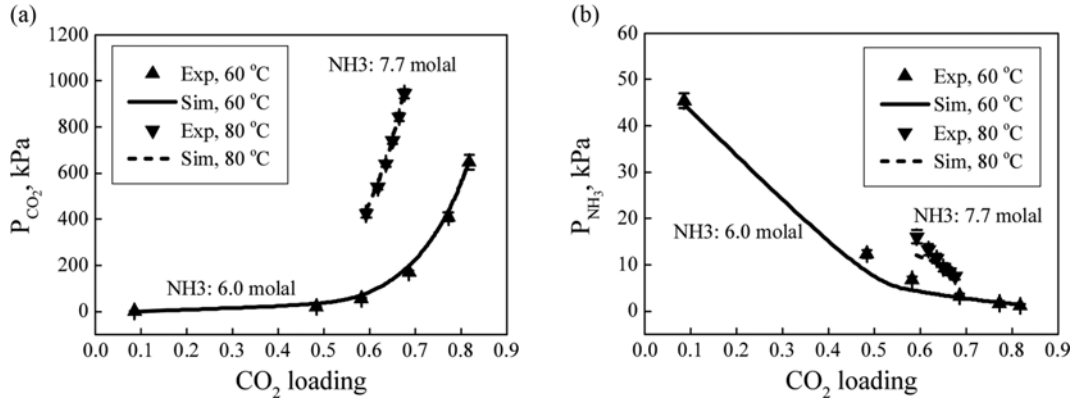

Fig. 3. Comparison of the predicted (a) CO_2 and (b) NH_3 partial pressures at 60 °C and 80 °C in the NH_3-CO_2-H_2O system and the experimental results reported by Kurz et al. [41] for 60 °C and Goppert and Maurer [42] for 80 °C.

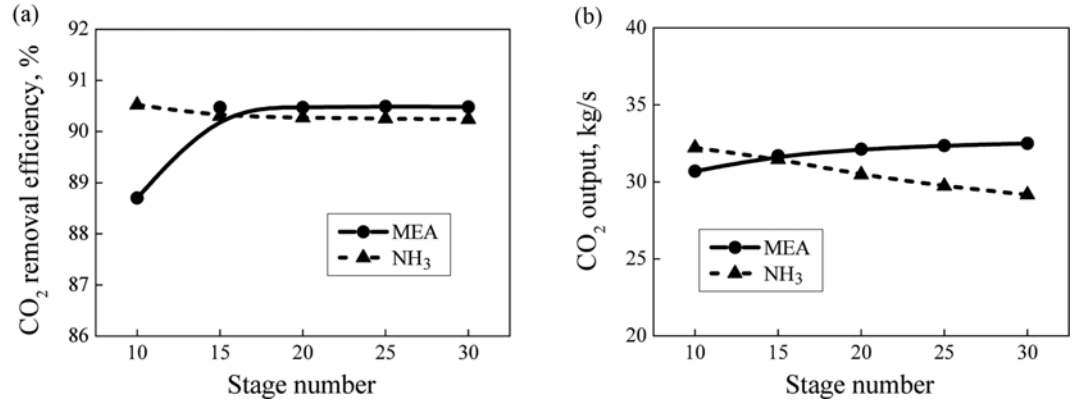

Fig. 4. The predicted (a) CO_2 removal efficiency and (b) CO_2 output in the MEA and NH_3 based large-scale CO_2 capture processes at different stage numbers.

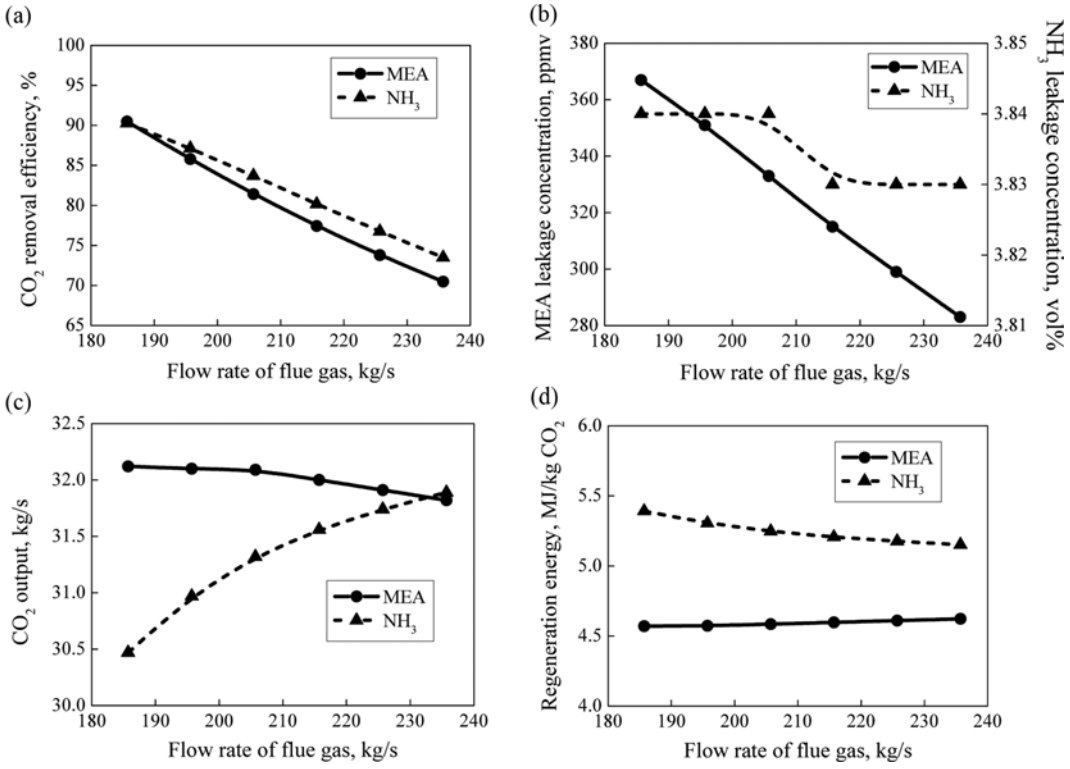

Fig. 5. Effects of the flow rate of the flue gas on the MEA and NH_3 based large-scale CO_2 capture processes: (a) CO_2 removal efficiency, (b) MEA and NH_3 leakage concentrations, CO_2 output, and (d) regeneration energy.

stage number. When the stage number reaches equal to or above 20, the predicted CO_2 removal efficiency and CO_2 output change little. Thus, in this paper, the absorber and stripper both adopt 20 stages when carrying out rate-based simulations.

RESULTS AND DISCUSSION

1. Effects of Flow Rate of Flue Gas

Effects of flow rate of the flue gas on the MEA and NH_3 based large-scale CO_2 capture processes are shown in Fig. 5. With the flow rate of the flue gas increasing, the CO_2 removal efficiencies for the two processes both decrease gradually, which is due to the limitation of the absorption capacity of the absorbent. When the flow rate of the flue gas is higher than 185.7 $kg \cdot s^{-1}$, the CO_2 removal efficiencies for the two processes are both lower than 90%. CO_2 removal efficiency for the MEA based process decreases more rapidly. Through calculating the CO_2 absorption rate in the absorber, we find that the CO_2 absorption rate for the MEA based process decreases, while that for the NH_3 based process increases with the flow rate of the flue gas increasing. This results in that the CO_2 output for the MEA based process decreases with the flow rate of flue gas increasing, while the CO_2 output for the NH_3 based process increases gradually. Considering that the reboiler heat duties change little, the CO_2 regeneration energy for the MEA based process increases with the flow rate of the flue gas increasing, while that for the NH_3 based process decreases gradually. But in this calculation, the CO_2 regeneration energy for the MEA based process is always lower than that for the NH_3 based process, where the CO_2 regeneration energy is the ratio of the reboiler heat duty to the CO_2 output. This is because for the stripper, more than half of the regeneration energy is used for heating the rich solvent [15], and the flow rate of the MEA solution is significantly lower than that of the aqueous ammonia. As the increased flue gas dilutes the slipping MEA and NH_3, the MEA and NH_3 leakage concentrations both decrease with the flow rate of the flue gas increasing. Also, the MEA leakage concentration (280-370 ppmv) is far lower than the NH_3 leakage concentration (3.83-3.84 vol%) and the NH_3 abatement system should be added for dealing with the NH_3 slip.

In general, for the MEA and NH_3 based large-scale CO_2 capture processes, the increase of the flow rate of the flue gas leads to the decrease of CO_2 removal efficiencies and absorbent leakage concentrations. With the flow rate of flue gas increasing, the CO_2 output decreases and the CO_2 regeneration energy increases for the MEA based process, while the CO_2 output increases and the CO_2 regeneration energy decreases for the NH_3 based process.

2. Effects of Temperature of Flue Gas

Effects of temperature of the flue gas on the MEA and NH_3 based large-scale CO_2 capture processes are shown in Fig. 6. The absorptions of CO_2 with MEA and NH_3 can both release heat. In theory, the increase of the temperature of the flue gas can inhibit the CO_2 absorption. But for the MEA and NH_3 based large-scale CO_2 capture processes, their liquid gas ratios are both very high, especially that of the NH_3 based process. This results in that the temperature in the absorber is mainly controlled by the temperature of the corresponding absorbent, rather than that of the flue gas. Thus, with the temperature of the flue gas increasing, the CO_2 removal

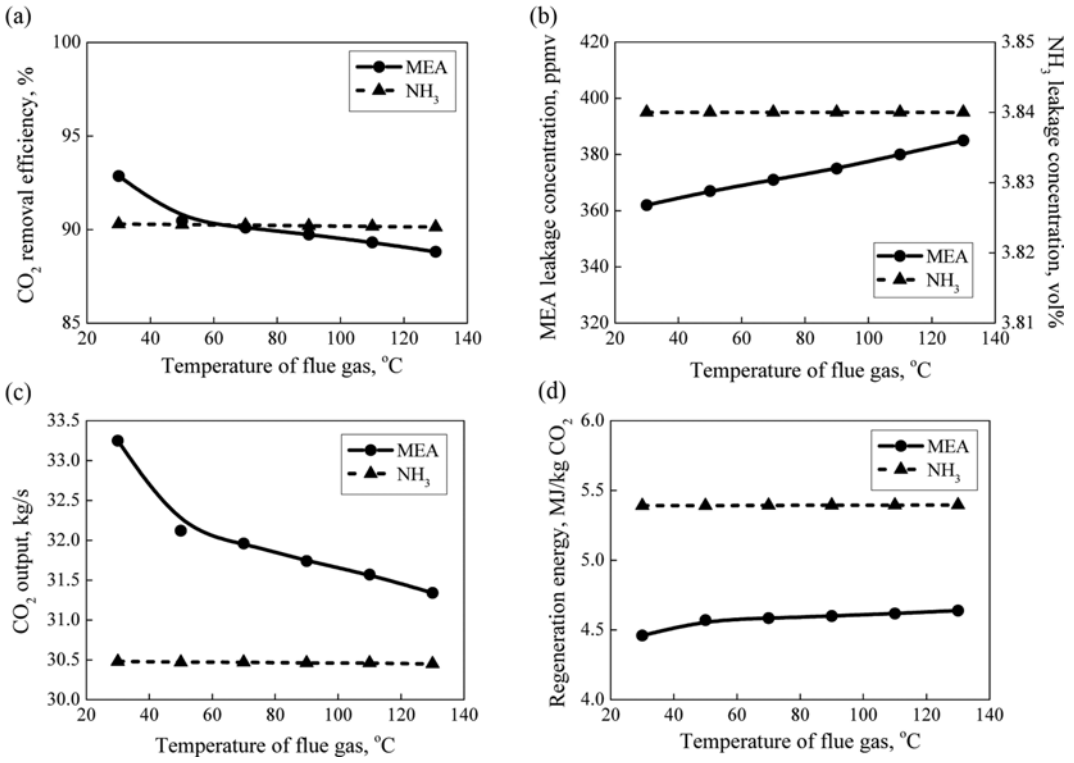

Fig. 6. Effects of the temperature of the flue gas on the MEA and NH_3 based large-scale CO_2 capture processes: (a) CO_2 removal efficiency, (b) MEA and NH_3 leakage concentrations, CO_2 output, and (d) regeneration energy.

efficiency for the MEA based process decreases slightly, while that for the NH_3 based process changes little, and at the same time the MEA leakage concentration increases slightly, while the NH_3 leakage concentration changes little. When the temperature of the flue gas is above 70 °C, the CO_2 removal efficiency for the MEA based process is already below 90%. The slight decrease of the CO_2 removal efficiency for the MEA based process with the temperature of the flue gas leads to the decrease of the CO_2 output and the increase of the CO_2 regeneration energy due to that the reboiler heat duty changes little.

In general, the liquid gas ratios of the MEA and NH_3 based large-scale CO_2 capture processes are very high, especially that for the NH_3 based process. For this reason, the temperature of the flue gas slightly affects the MEA based process; and the CO_2 removal efficiency and CO_2 output decrease slightly with the increase of the temperature of the flue gas while the MEA leakage concentration and CO_2 regeneration energy increase slightly. Meanwhile, the temperature of the flue gas almost does not affect the NH_3 based process. From the perspective of the exhaust system of the power plants, higher exhausted flue gas means lower requirement for the cooling operations at the pretreatment stage of the flue gas. MEA solution is easier degraded at higher temperatures [43], and the increase of the temperature of the flue gas can reduce the CO_2 absorption capacity of the MEA solution. On the contrary, the NH_3 based CO_2 capture process does not have the degradation problem.

3. Effects of CO_2 Concentration of Flue Gas

Effects of CO_2 concentration of the flue gas on the MEA and NH_3 based large-scale CO_2 capture processes are shown in Fig. 7. Keeping the absorbents for the two processes unchanged, with the CO_2 concentration of the flue gas increasing, the CO_2 removal efficiencies for the two processes decrease gradually and the CO_2 removal efficiency for the MEA based process decreases more rapidly. When the CO_2 concentration of the flue gas is lower than 10.5 vol%, the decrease of the CO_2 removal efficiency for the MEA based process is slow, but when the CO_2 concentration is higher than 10.5 vol%, it begins to decrease significantly. When the CO_2 concentration is higher than 12.5 vol%, the CO_2 removal efficiency for the MEA based process is smaller than that for the NH_3 based process. Although the CO_2 removal efficiencies for the two processes decrease gradually, the CO_2 absorption rates for the two processes both increase with the CO_2 concentration of the flue gas increasing. The increase of CO_2 absorption rate means higher CO_2 loading of the rich solvent flowing out of the absorber. As the rich solvent directly flows into the stripper after the heat-exchanger and heater, higher CO_2 loading of the rich solvent can lead to the increase of the CO_2 output, and therefore, the CO_2 outputs for the two processes increase gradually. Considering the reboiler heat duty changes little, the increase of the CO_2 outputs for the two processes lead to the decrease of their CO_2 regeneration energies. Besides, the increases of the CO_2 absorption rates for the two processes mean that the heat due to the absorption of CO_2 increases. Compared with the NH_3 based CO_2 capture process, the released heat due to the absorption of CO_2 with MEA is higher and the liquid gas ratio for the MEA based process is lower, the MEA leakage concentration increases more significantly due to the increase of the released heat for absorption.

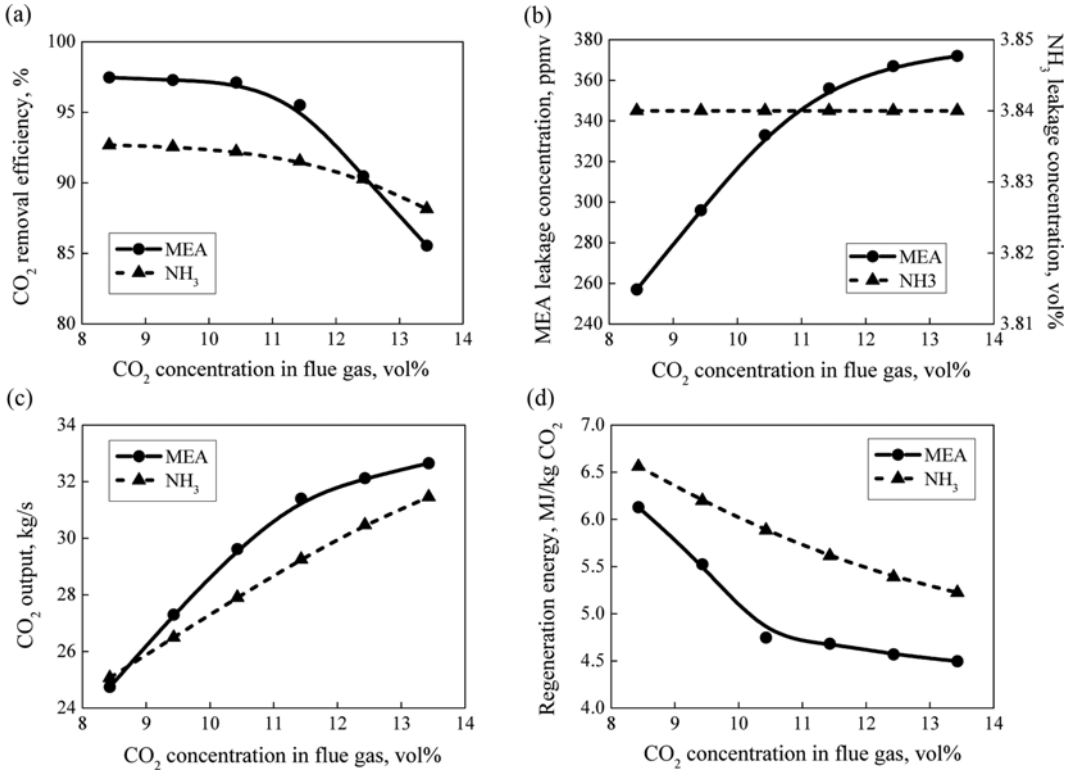

Fig. 7. Effects of the CO_2 concentration in flue gas on the MEA and NH_3 based large-scale CO_2 capture processes: (a) CO_2 removal efficiency, (b) MEA and NH_3 leakage concentrations, CO_2 output, and (d) regeneration energy.

In general, with the CO_2 concentration of the flue gas increasing, for the MEA and NH_3 based large-scale CO_2 capture processes, the CO_2 removal efficiencies decrease, the absorbent leakage concentrations increase, the CO_2 outputs increase, and the CO_2 regeneration energies decrease. Compared with the MEA based process, the decrease of the CO_2 removal efficiency and the CO_2 regeneration energy and the increase of the NH_3 leakage concentration and the CO_2 output are all smaller for the NH_3 based CO_2 capture process.

CONCLUSIONS

Rate-based models for the MEA and NH_3 based large-scale CO_2 capture processes were established, respectively. By the rate-based process simulating, effects of the parameters of the flue gas such as its flow rate, temperature and CO_2 concentration on the absorption and regeneration processes of the large-scale CO_2 capture in packed columns using MEA solution and aqueous NH_3 were investigated.

The increase of the flow rate of the flue gas leads to the decrease of CO_2 removal efficiencies and absorbent leakage concentrations for the two processes. With the flow rate of flue gas increasing, the CO_2 output decreases and the CO_2 regeneration energy increases for the MEA based process, while the CO_2 output increases and the CO_2 regeneration energy decreases for the NH_3 based process. The temperature of the flue gas slightly affects the MEA based process, and the CO_2 removal efficiency and CO_2 output decrease slightly with the increase of the temperature of the flue gas, while the MEA leakage concentration and CO_2 regeneration energy increase slightly. But, the temperature of the flue gas almost does not affect the NH_3 based process. From the perspective of the exhaust flue gas system of the power plants, high temperature of the exhausted flue gas means low requirement for the cooling operations at the pretreatment stage of the flue gas, which is more favorable for the NH_3 based CO_2 capture process. For both of the MEA and the NH_3 based CO_2 capture processes, with the CO_2 concentration of the flue gas increasing, the CO_2 removal efficiencies and the CO_2 regeneration energies decrease, the absorbent leakage concentrations and the CO_2 outputs increase.

ACKNOWLEDGEMENTS

This work was supported by the National Natural Science Foundation of China under Grant No. 51390493, and the Beijing Municipal Commission for Science & Technology under Grant No. Z08040902950803.

REFERENCES

1. B. T. Zhao, Y. X. Su and Y. C. Peng, *Int. J. Greenh. Gas Control*, **17**, 481 (2013).
2. N. Razi, H. F. Svendsen and O. Bolland, *Int. J. Greenh. Gas Control*, **19**, 331 (2013).
3. S. Y. Park, K. B. Yi, C. H. Ko, J. H. Park, J. N. Kim and W. H. Hong, *Energy Fuels*, **24**, 3704 (2010).
4. B. Huang, S. S. Xu, S. W. Gao, L. B. Liu, J. Y. Tao, H. W. Niu, M. Cai and J. Cheng, *Appl. Energy*, **87**, 3347 (2010).

5. P. Galindo, A. Schaffer, K. Brechtel, S. Unterberger and G. Scheffknecht, *Fuel*, **101**, 2 (2012).
6. Q. Zeng, Y. C. Guo, Z. Q. Niu and W. Y. Lin, *Ind. Eng. Chem. Res.*, **50**, 10168 (2011).
7. C. K. Ahn, H. W. Lee, Y. S. Chang, K. Han, J. Y. Kim, C. H. Rhee, H. D. Chun, M. W. Lee and J. M. Park, *Int. J. Greenh. Gas Control*, **5**, 1606 (2011).
8. V. Darde, W. J. M. van Well, P. L. Fosboel, E. H. Stenby and K. Thomsen, *Int. J. Greenh. Gas Control*, **5**, 1149 (2011).
9. J. T. Yeh, K. P. Resnik, K. Rygle and H. W. Pennline, *Fuel Process. Technol.*, **86**, 1533 (2005).
10. B. G. Choi, G. H. Kim, K. B. Yi, J. N. Kim and W. H. Hong, *Korean J. Chem. Eng.*, **29**(4), 478 (2012).
11. K. Han, C. K. Ahn, M. S. Lee, C. H. Rhee, J. Y. Kim and H. D. Chun, *Int. J. Greenh. Gas Control*, **14**, 270 (2013).
12. AspenTech, *Aspen Plus document version V7.3*, AspenTech, Burlington, Massachusetts (2011).
13. L. Q. Duan, Y. Yang, S. H. Zhang and Y. P. Yang, *J. N. Chin. Electr. Power Univ.*, **39**(1), 7 (2012).
14. M. K. Zhang and Y. C. Guo, *Int. J. Greenh. Gas Control*, **16**, 61 (2013).
15. H. Yu, L. C. Li, S. Morgan, A. Allport, A. Cottrell, J. Mcgregor, L. Wardhaugh and P. Feron, In: Chemeca 2012, Wellington, 1097 (2012).
16. Y. Zhang, H. Chen, C. C. Chen, J. M. Plaza, R. Dugas and G. T. Rochelle, *Ind. Eng. Chem. Res.*, **48**, 9233 (2009).
17. A. Ghaemi, S. Shahhosseini and M. G. Maragheh, *Chem. Eng. J.*, **149**, 110 (2009).
18. G. Puxty, R. Rowland and M. Attalla, *Chem. Eng. Sci.*, **65**, 915 (2010).
19. N. Dave, T. Do, G. Puxty, R. Rowland, P. H. M. Feron and M. I. Attalla, *Energy Procedia*, **1**, 949 (2009).
20. C. H. Hsu, H. Chu and C. M. Cho, *J. Air Waste Manage. Assoc.*, **53**, 246 (2003).
21. A. C. Yeh and H. Bai, *Sci. Total Environ.*, **228**, 121 (1999).
22. Z. Q. Niu, Y. C. Guo and W. Y. Lin, *J. Chem. Eng. Chin. Univ.*, **24**(3), 514 (2010).
23. G. Pellegrini, R. Strube and G. Manfrida, *Energy*, **35**, 851 (2010).
24. S. C. Ma, M. X. Wang, Y. X. Sun, J. W. Cui and W. Z. Chen, *J. Chin. Soc. Power Eng.*, **32**(1), 52 (2012).
25. R. Rivera-Tinoco and C. Bouallou, *J. Cleaner Prod.*, **18**, 875 (2010).
26. M. K. Zhang and Y. C. Guo, *Appl. Energy*, **111**, 142 (2013).
27. Z. Q. Niu, Y. C. Guo and W. Y. Lin, *Proc. CSEE*, **30**(32), 41 (2010).
28. S. C. Ma, Y. X. Sun, Y. Zhao, W. W. Fang, J. Han and P. Z. Liang, *Acta Chim. Sinica*, **69**(12), 1469 (2011).
29. D. H. V. Wagener and G. T. Rochelle, *Chem. Eng. Res. Des.*, **89**, 1639 (2011).
30. X. Z. Zeng, C. H. Chen and B. C. Gao, *Environ. Prot. Chem. Ind.*, **20**(6), 12 (2000).
31. P. M. Mathias, S. Reddy and J. P. O'Connell, *Int. J. Greenh. Gas Control*, **4**, 174 (2010).
32. M. K. Zhang and Y. C. Guo, *Int. J. Greenh. Gas Control*, **29**, 22 (2014).
33. E. Chen, *Carbon dioxide absorption into piperazine promoted potassium carbonate using structured packing*, Ph. D. Thesis, University of Texas at Austin, Austin, Texas (2012).
34. T. H. Chilton and A. P. Colburn, *Ind. Eng. Chem. Res.*, **26**, 1183 (1934).
35. J. L. Bravo, J. A. Rocha and J. R. Fair, *Hydrocarbon Process.*, **64**, 91 (1985).
36. Z. Q. Niu, Y. C. Guo, Q. Zeng and W. Y. Lin, *Fuel Process. Technol.*, **108**, 154 (2013).
37. B. R. Pinsent, L. Pearson and F. J. W. Roughton, *Trans. Faraday Soc.*, **52**, 1512 (1956).
38. H. Hikita, S. Asai, H. Ishikawa and M. Honda, *Chem. Eng. J.*, **13**, 7 (1977).
39. J. I. Lee, F. D. Otto and A. E. Mather, *J. Appl. Chem. Biotechnol.*, **26**, 541 (1976).
40. F. Y. Jou, A. E. Mather and F. D. Otto, *Can. J. Chem. Eng.*, **73**, 140 (1995).
41. F. Kurz, B. Rumpf and G. Maurer, *Fluid Phase Equilib.*, **104**, 261 (1995).
42. U. Goppert and G. Maurer, *Fluid Phase Equilib.*, **41**, 153 (1988).
43. C. Gouedard, D. Picq, F. Launay and P. L. Carrette, *Int. J. Greenh. Gas Control*, **10**, 244 (2012).